Available online at www.sciencedirect.com

ScienceDirect

Proceedings of the Combustion Institute 37 (2019) 5473–5480

Proceedings of the Combustion Institute

www.elsevier.com/locate/proci

A reactive molecular dynamics simulation study of methane oxidation assisted by platinum/graphene-based catalysts

Muye Feng, Xi Zhuo Jiang, Kai H. Luo*

Department of Mechanical Engineering, University College London, Torrington Place, London WC1E 7JE, UK

Received 29 November 2017; accepted 26 May 2018
Available online 21 June 2018

Abstract

Platinum-decorated functionalized graphene sheet (Pt@FGS) is a promising nanoparticle additive for catalytic fuel combustion. In this study, four cases involving pure methane oxidation and methane oxidation in the presence of various Pt/graphene-based nanoparticle catalysts are investigated using the reactive force field molecular dynamics (ReaxFF MD) simulations to reveal catalytic mechanisms and kinetics of methane oxidation. The results demonstrate that Pt@FGS is the most effective catalyst among all the nanoparticle candidates involved in this research. Compared with pure methane oxidation, the combination of Pt and FGS in the Pt@FGS reaction improves the catalytic activity by dramatically lowering the activation energy by approximately 73%. Additionally, the catalytic methane oxidation is initiated by the cleavage of C–H bond and the production of hydroxyl. The observed H transfer process suggests that enhanced dehydrogenation of Pt@FGS and interatomic exchanges activate the catalytic cycle and dominate the catalytic process. Moreover, FGS can be further oxidized mostly at the edge of the sheet to increase the functionality. In summary, this research sheds light on the catalytic mechanisms for enhanced fuel combustion in the presence of Pt@FGS.

Keywords: Methane oxidation; Platinum/graphene-based catalyst; Molecular Dynamics (MD) simulation; Reactive force field (ReaxFF)

1. Introduction

Graphene, a one-layer honeycomb carbon material extensively applied in a wide range of areas, is well known as the first two-dimensional atomic crystal possessing many extraordinary properties such as extreme mechanical strength, high thermal and excellent electronic conductivity [1,2]. Graphene-based materials decorated with metal nanoparticles [3,4] or functional groups [5] have been recently considered as effective catalysts for fuel combustion. Functionalized Graphene Sheet (FGS), a representative of the effective catalysts, can enhance the reaction mainly due to its diverse active sites. The advantages of adding nano-sized metal particles into the fuel include increasing energy density, shortening ignition delay and improving burning rates [6,7]. Therefore, it is of

* Corresponding author.
E-mail address: k.luo@ucl.ac.uk (K.H. Luo).

https://doi.org/10.1016/j.proci.2018.05.109

great interest to study the metal-decorated functionalized graphene sheet as a novel catalyst for fuel and propellant combustion. Platinum (Pt) is recognized as an effective metal catalyst for promoting oxidation of hydrocarbons [8,9] and resisting sulphur poisoning in exhaust gas after-treatment [10]. Successful synthesis of Pt-graphene composite [4,11] lays the foundation for improving fuel combustion in the presence of Pt-decorated functionalized graphene sheet (Pt@FGS). Methane, the primary component of natural gas, is one of the cleanest and most ideal alternatives to other fossil fuels. The low carbon/hydrogen ratio of methane contributes to considerable reduction of carbon dioxide emissions. Additionally, the heat sink capacity and specific energy content of methane are high [12]. In recent years, there has been increasing interest in using methane as a propellant for reusable boosters and rocket engines, where combustion takes place at extremely high temperatures and pressures [13]. However, the greatest C–H bond strength (with an $H–CH_3$ bond dissociation energy of 104 kcal/mol) among all the saturated hydrocarbons causes unsatisfactory gas phase combustion performance [14]. To improve combustion performance, Pt@FGS may be added to the methane/air system as a catalyst.

Liu et al. [15] employed the ab initio molecular dynamics (MD) simulations to study the enhanced thermal decomposition of nitromethane on FGS and demonstrated that the catalytic activity (CA) originates from lattice defect complex within the graphene sheet. Zhang et al. [16] also conducted a research on self-enhanced CA of FGS in the combustion of nitromethane by a reactive force field (ReaxFF) MD simulation method and obtained similar results. The findings from these two studies have been validated by Sabourin et al.'s experiment, which found that the addition of FGS in nitromethane increased the burning rate up to 175% over neat nitromethane and outperformed more conventional additives such as aluminium monohydroxide and silica nanoparticles [5]. Sim [17] explored the thermal and catalytic decomposition of n-dodecane with Pt/graphene-based catalysts both experimentally and computationally (ReaxFF MD simulation). These results mutually validate each other.

Experiments have proved graphene-based materials to be good catalysts, but the underlying mechanisms are difficult to be determined by the existing experimental techniques. MD is a promising method to investigate the detailed oxidation reactions at the atomic level. Quantum Mechanics (QM) methods can provide high accuracy for small systems (typically less than 100 atoms) but are computationally very expensive for studying the full dynamics of large systems. Classic MD using empirical force fields allow large scale simulations (involving millions of atoms) but are usually not applicable for chemical reactions. The ReaxFF MD method based on the bond order concept is able to model dissociation, transition and formation of chemical bonds within a reactive system, which bridges the gap between the above two approaches [18]. It is computationally cost-efficient to simulate a large reactive system for a long time while retaining a high level of accuracy. More details of the ReaxFF formalism and development can be found in previous articles [18–20]. Also, many ReaxFF force fields were developed specifically to study the hydrocarbon systems with catalysts [21,22].

In this study, ReaxFF MD simulations are performed to study the fundamental catalytic mechanisms and kinetics of methane oxidation mixed with nanoparticle additives. By observing the atomic trajectory and analyzing evolutions of key species, major catalytic mechanisms are deduced. Following the first-order reaction model, the rate constant k is determined and then the Arrhenius Plot is drawn to calculate the activation energy (E_a) of each simulation case. Finally, the catalytic effect of all the nanoparticle additives are compared with each other.

2. Computational methods

The ReaxFF formulation implemented in LAMMPS (Large-scale Atomic/Molecular Massively Parallel Simulator) package [23], with ReaxFF force fields of C/H/O [19] and Pt/C/H/O [22] parameters are used for MD simulations. Four 3-dimensional periodic systems with different sizes are built at the same density of 0.0325 g/cm^3. This density relates to an initial gas phase pressure of about 30 atm, which is high enough to ensure that the reaction occurs at the ReaxFF MD simulation time scale. A representative stoichiometric condition is chosen to clarify the fundamental catalytic mechanisms and kinetics of methane oxidation and its mixture with various nanoparticle catalysts. The base system contains 50 CH_4 and 100 O_2 gas phase molecules (initial equivalence ratio of 1), and the other three systems include three specific catalysts, i.e. a Functionalized Graphene Sheet (FGS), two Tetrahedral Pt Clusters (Pt) and a Pt-decorated Functionalized Graphene Sheet (Pt@FGS), respectively. The C/H/O force field is used for the systems of pure CH_4/O_2 and with FGS, while the Pt/C/H/O force field is used for the systems with Pt and with Pt@FGS. It is appropriate to use a different force field because the interaction of each atom type pair is changed with the introduction of the Pt element. The details of system construction and structure of each catalyst are illustrated in the supplemental material (Fig. S1). More specifically, a pristine graphene sheet (PGS) with 1269 carbon atoms is modified for FGS (Fig. S1b). Totally 16 identical functional groups are implanted in the PGS resulting in a carbon to oxygen (C/O) ratio of 13. Each functional group

contains a divacancy decorated by two ethers with 4 additional hydroxyls attached to C atoms nearby [15]. With respect to the Pt@FGS (Fig. S1d), two tetrahedral Pt clusters are adsorbed on the two single-vacancies in a triangle contact way, which was found to be the most stable form from DFT calculations [24,25]. It is believed that for such a small system, using a tetrahedral Pt cluster instead of a larger one is appropriate to study the combined catalytic activity of Pt and FGS. Otherwise, the catalytic reaction would be dominated by the large Pt cluster within this small system rather than showing the combined effect of Pt and FGS. For the system of CH_4/O_2 with Pt@FGS (Fig. S1d), the periodic box is cubic and the side length is 60 Å. To keep the density constant, the z-axial length of the box for the other three systems is varied, while other parameters remain the same. The volumes of the catalysts are evaluated by creating a Conolly surface assigned with a Conolly radius of 1.0 Å.

The canonical ensemble (NVT) is adopted for all the MD simulations. Every simulation begins with energy minimization via conjugate gradient algorithm to eliminate artificial effects of the structure. The system temperature is maintained by the Nosé-Hoover thermostat with a damping constant of 50 fs. Both ramped-temperature and fixed-temperature NVT MD simulations are performed to study the methane oxidation. Each simulation system is equilibrated at the starting temperature for 100 ps with a time step of 0.1 fs. Especially for those fixed-temperature simulations starting from a high temperature (higher than 1000 K), C–O and H–O bond parameters are switched off by eliminating the bond parameters describing these interactions in the force field to prevent the occurrence of reactions during the equilibration [19]. Pt-O and Pt-H bond parameters are also turned off in the equilibrium of the systems involving Pt element. It is noteworthy that catalysts containing FGS (i.e. FGS and Pt@FGS) and surrounding gas molecules are equilibrated separately at high temperatures so that the structures of those catalysts could remain intact. After the equilibrium, a series of MD simulations are carried out for 4000 ps (ramped-temperature simulations) or 1000 ps (fixed-temperature simulations) with a time step of 0.2 fs. In previous ReaxFF MD simulations, particularly for combustion, employing a high temperature to accelerate the reactions is a common strategy to overcome the limitation of computing power [14,19,26–29]. More importantly, the present research is a comparative study of different cases, so the absolute temperature used is less important. A 0.2 bond order cutoff is employed to recognize the molecules and analyze the species forming during the simulation. A low cutoff value could help with capturing all the reactions in order to detect all possible reaction pathways including those unsuccessful events producing very short-lived species in low-density simulations [19,27]. For each fixed-temperature simulation case, results of three replicas with unique starting configurations are averaged for further analysis. All the visualizations in this study are produced by Visual Molecular Dynamics (VMD) software [30].

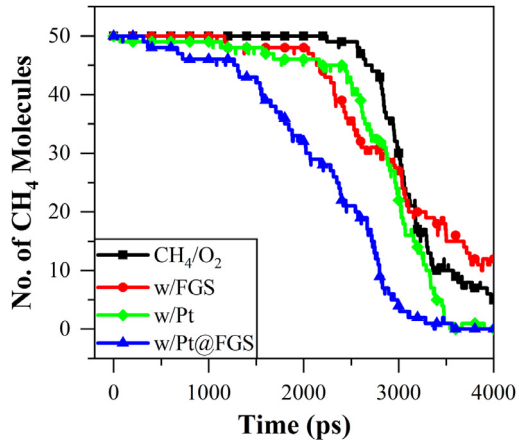

Fig. 1. Time evolution of CH_4 molecule number for systems with different catalysts during temperature ramping NVT MD simulations from 300 to 3000 K.

3. Results and discussions

3.1. Reaction rate and time evolution of key species

The temperature ramping NVT MD simulations from 300 to 3000 K with heating rate of 0.90 K/ps are performed to investigate the reaction rate and mechanisms of methane oxidation mixed with catalytic nanoparticles. An additional 1000 ps simulation at the constant temperature of 3000 K is appended to the 3000 ps simulation for further consumption of CH_4 as shown in Fig. 1.

In Fig. 1, the fastest reaction rate of Pt@FGS case suggests that Pt@FGS has the most remarkable catalytic effect on methane oxidation among all the nanoparticle candidates. In contrast, FGS does accelerate the methane consumption to some extent, but hinders the oxidation at the late stage of the reaction. Moreover, the results show that the reaction rate of Pt is significantly quicker than FGS after about 3000 ps but is slightly slower than FGS before that time point. In this research, methane molecules are observed to be adsorbed on the graphene-containing nanoparticles at low temperatures (~300–600 K), which is consistent with previous experimental [31] and computational [32] studies. The time evolution of some key species is shown in the supplemental material (Figs. S2 and S3). After the initial equilibration and when CH_4 starts to decay, the first drop in the number of CH_4

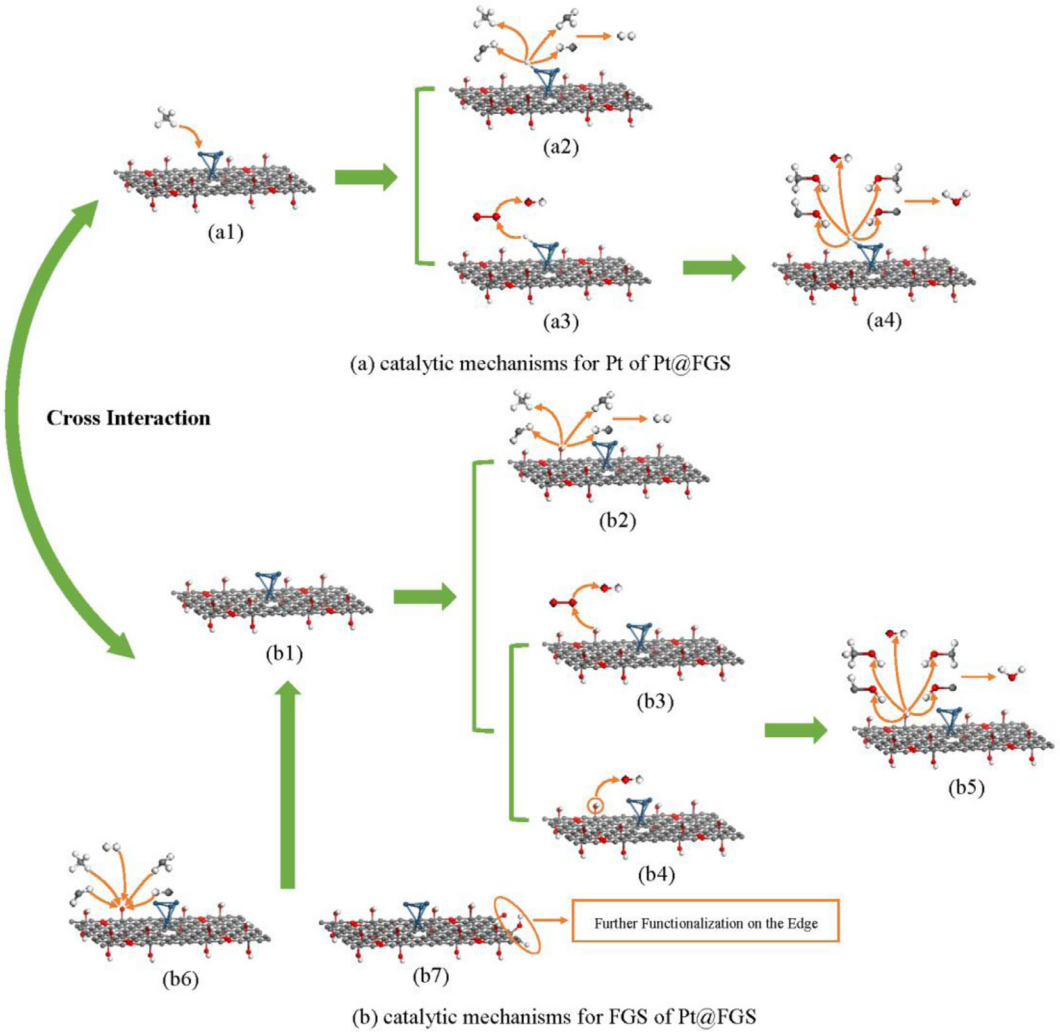

Fig. 2. Proposed overall catalytic mechanism for methane oxidation catalysed by Pt@FGS: catalytic mechanisms for (a) Pt and (b) FGS. C, H, O and Pt atoms are represented in black, white, red and blue, respectively. (a1–a4) demonstrate the dehydrogenation of CH_4 on Pt (a1) followed by the H radical participating in either H_2 (a2) or H_2O (a3, a4) formation related reactions, while (b1–b7) illustrate the OH functional groups on FGS (b1) contributing to the production of H_2 (b2) and H_2O (b3–b5), and show the recovery of the OH functional group on FGS (b6) as well as the increased functionality at the edge of the graphene (b7). The integrated Pt and FGS combines the catalytic mechanisms of (a) and (b) and the two catalytic cycles interact with each other. (For interpretation of the references to color in this figure legend, the reader is referred to the web version of this article.)

molecules in the FGS system is observed due to direct dehydrogenation of CH_4 on FGS. For the Pt and Pt@FGS systems, the CH_4 molecule is firstly adsorbed on the Pt surface at the end of the equilibration and then dehydrogenated by the Pt cluster.

3.2. *Catalytic mechanisms of methane oxidation with Pt/graphene-based catalysts*

Based on the analysis of species and the observation of atomic trajectories, major catalytic mechanisms concerning interatomic exchange can be deduced as shown in Fig. 2.

3.2.1. *Catalytic mechanisms of methane oxidation with Pt and FGS*

Firstly, Pt is known to be capable of accelerating dehydrogenation of hydrocarbons to yield hydrogen [9,33,34]. Specifically in the present study, an H radical of CH_4 molecule is adsorbed on the Pt surface (Fig. 2a1) followed by the H radical participating in subsequent reactions. The H radical can abstract another H radical from CH_4 molecule

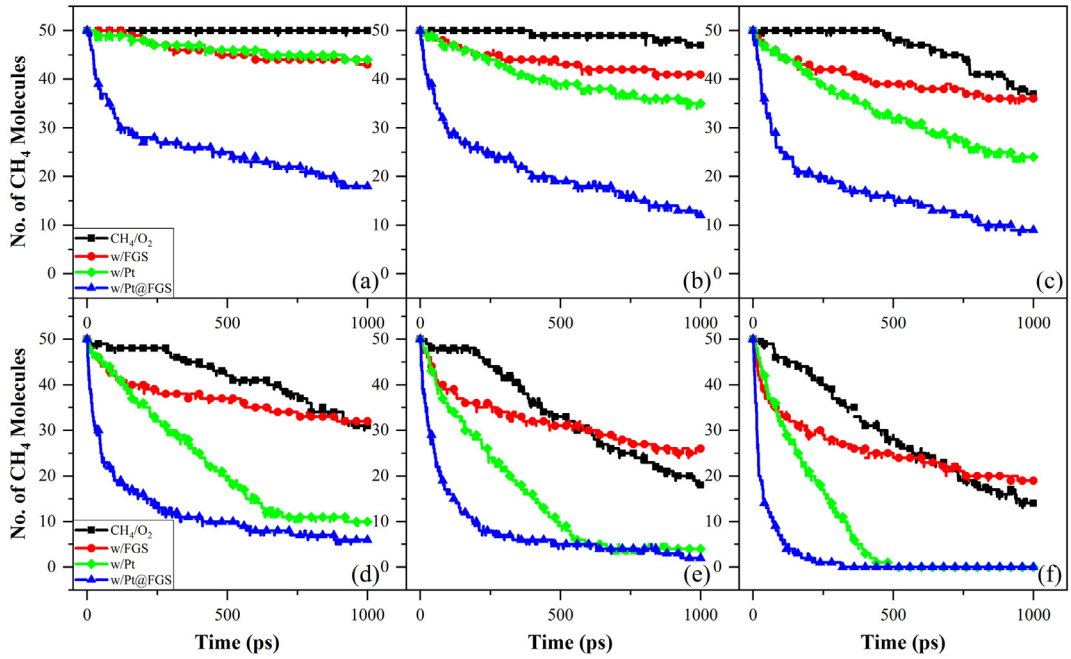

Fig. 3. Time evolution of CH_4 molecule number for systems with different catalysts at the same temperature during fixed-temperature NVT MD simulations ranging from 2000 to 3000 K: (a) 2000 K, (b) 2200 K, (c) 2400 K, (d) 2600 K, (e) 2800 K and (f) 3000 K.

or other hydrocarbon radicals like CH_3 or CH_2 to form a hydrogen molecule (Fig. 2a2). Also, this H radical can interact with the O radical from the O_2 molecule, forming an OH radical (Fig. 2a3). In turn, both free OH radical and the OH group from intermediate reaction products like CH_3OH or CH_2OH tend to attract the H radical adsorbed on the Pt surface forming a water molecule (Fig. 2a4). These observed catalytic mechanisms were also reported in previous experimental [35,36] and computational [37,38] studies. Similarly, in the FGS case, the hydroxyl functional group contributes an H radical to the formation of hydrogen and water molecules (Fig. 2b2–b5). However, some hydroxyl groups are found to be detached from the graphene sheet (Fig. 2b4) during reactions generating more hydroxyl radicals, which could participate in the reaction. Afterwards, another H radical, usually from the methane molecule or other hydrocarbon radicals, is adsorbed on the O atom (hydroxyl group which loses the H radical) attached to the graphene sheet recovering to a hydroxyl group (Fig. 2b6). Then this hydroxyl group undergoes the same process again. Additionally, the graphene sheet is further oxidized to increase the functionality, especially at the edge of the graphene (Fig. 2b7), which can also be confirmed by the more rapid O_2 consumption of FGS and Pt@FGS compared to pure CH_4/O_2 and Pt in Fig. S2. Only a few O radicals are observed adhering on

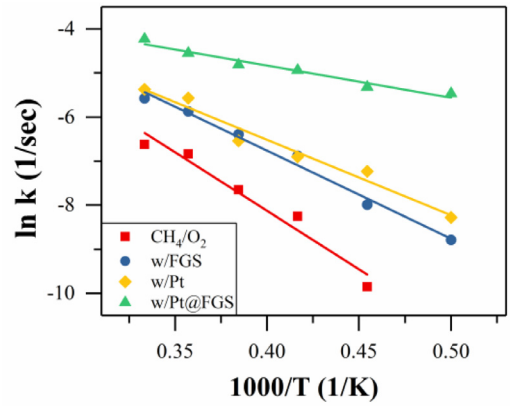

Fig. 4. Arrhenius Plot: determination of activation energy for methane oxidation and its mixture with various nanoparticle additives.

the internal defect-free C atoms later and the sheet structure is retained during the whole simulation period, which agrees with the previous simulation results [16]. The attachment of H and OH radicals to defect-free C atoms is occasional and does not last long. Instead, these radicals react with other intermediate species frequently. The catalytic cycle starting from the H transfer process repeats after the functionalization. Thus, the original active sites

on the FGS can be considered as the internal edge of the graphene sheet. Similar mechanism is also corroborated by previous studies [15,16,39].

3.2.2. Catalytic mechanisms of methane oxidation with Pt@FGS

The integrated Pt and FGS shows the most outstanding catalytic performance, which can be attributed to the combined catalytic mechanisms of Pt and FGS. Fig. 2 depicts the overall catalytic mechanism for methane oxidation catalysed by Pt@FGS. The two Pt clusters and functional groups on the FGS conduct the H transfer process simultaneously. Each of the two processes forms a catalytic cycle. Briefly, the H radical adsorbed on the Pt surface or from the hydroxyl on FGS interacts with the H-containing intermediates producing a H_2 molecule. In turn, the OH group from this particular H radical abstracted by the O radical from the O_2 molecule, the hydroxyl partitioned from the graphene sheet or all the OH-containing products, can react, as feedback, with the H radical on the Pt surface or H radical on hydroxyl of FGS to form water. Besides, the graphene sheet is further oxidized to enhance the functionality, enabling more functional groups to participate in the catalytic reactions. After losing the H radical, the Pt and the O atoms attached on graphene sheet adsorb another H radical from the H-containing species, which drives the catalytic cycle. Moreover, the intermediate products of either cycle could also interact with each other, thereby increasing the CA. These findings suggest that the improved CA is attributed to the acceleration of interatomic exchange, rather than the creation of new reactions to form new species. The branching ratios for some important competing pathways are determined by analyzing the atomic trajectory and evolution of species together and the results are shown in Table S1 in the supplemental material. Fig. S2 shows that CH_3 and OH radicals appear at the initial stage of the reaction (when CH_4 starts to decay) and subsequently disappear fast as the number of CH_4 molecules decreases. This phenomenon indicates that methane oxidation is initiated by the cleavage of C–H bond and catalytic production of hydroxyl. In addition, the extremely short lifetime of H radical validates the rapid H transfer process during the reaction. The main methane oxidation products are CO_2 and H_2O, which is consistent with the conventional methane oxidation without catalysts. A number of H_2 molecules are also observed during the reaction because both pyrolysis of methane and dehydrogenation of methane over catalysts can generate hydrogen under high temperature [40,41]. Importantly, all the graphene structures are monitored and their structures are retained throughout the whole simulation period. However, it is noteworthy that most active sites of Pt@FGS are consumed eventually leaving the structure like a PGS but most active sites of FGS are retained at the end of the simulation. This finding proves that the combination of Pt and FGS can further enhance the CA.

3.3. Global kinetics of methane oxidation with Pt/graphene-based catalysts

Figure 3 shows the CH_4 decay of systems with different catalysts over time within the temperature range from 2000 to 3000 K with an increment of 200 K. As expected, the consumption rate of CH_4 molecules is higher as temperature increases, which means that high temperature benefits the catalytic functions. Furthermore, in accordance with the results of temperature ramping MD simulations, Pt@FGS has the most significant catalytic effect on methane oxidation compared to other candidates. The bottom three panels confirm that FGS hinders the methane oxidation at the late stage of the reaction under high temperatures, which also agrees with the results shown in Fig. 1. Combing the aforementioned analysis of sheet structural differences between Pt@FGS and FGS during the simulation (end of the Section 3.2.2), it is believed that methane oxidation is impeded in the presence of FGS at the late stage of the reaction probably due to the limited activity of active sites on FGS during that time period. Due to this low catalytic activity, the reactions with FGS could compete with those with CH_4, leading to the slower methane oxidation.

According to the results of fixed-temperature NVT MD simulations shown in Fig. 3, the kinetics of pure methane oxidation and its mixtures with various catalysts can be studied. Following the first-order reaction model, the rate constant k at each temperature and E_a of the Arrhenius Equation (Eq. (1)) are determined for the four cases (as shown in Fig. 4).

$$\ln k = \ln A - (E_a/R) \cdot (1/T) \tag{1}$$

where k is the rate constant, A pre-exponential factor, E_a activation energy, R gas constant and T absolute temperature.

The calculated E_a for all these systems are summarized in Table 1. From Table 1, the descending order of E_a is: Pure CH_4/O_2 > with FGS > with Pt > with Pt@FGS. Pt@FGS reduces E_a dramatically by 72.53% compared with pure CH_4/O_2, which results from the combined CA of Pt and FGS. By contrast, the other two catalysts (FGS and Pt) lower the E_a of pure CH_4/O_2 by 24.79% and 35.54%, respectively. The results obtained from this research are also verified by previous studies (also summarized in Table 1), which proves the validity of the adopted ReaxFF MD simulation methodology. The difference in the overall activation energy determined by the present study and that reported in the literature is generally acceptable, considering the various different conditions applied (e.g. temperature, pressure, equivalence ratio, catalyst loading, catalyst structure, combustion

Table 1
Calculated activation energy for methane oxidation and its mixture with various nanoparticle additives and comparison with previous results from the literature.

System	Fitting formula (R^2)	E_a (kcal/mol)	
		study	literature
CH_4/O_2	$\ln k = 2.49–26529.82/T$ (0.96)	52.68	26.0–48.4 [43–45]
w/FGS	$\ln k = 1.22–19948.43/T$ (0.99)	39.62	N/A
w/Pt	$\ln k = 0.32–17099.41/T$ (0.97)	33.96	19.1–47.8 [46–48]
w/Pt@FGS	$\ln k = -1.92–7284.79/T$ (0.96)	14.47	N/A

environment, etc.) and uncertainties in both the numerical modelling and experiment. Although there is no straightforward comparison available for the systems with FGS and with Pt@FGS, some indirect evidence can be found. Sirijaraensre and Limtrakul [42] figured out an E_a of 28.2 kcal/mol for partial oxidation of methane to methanol over the graphene supported Au_4Pt nanocluster by DFT calculations. In addition, experimental research revealed that E_a for thermal and catalytic decomposition of n-dodecane (n-$C_{12}H_{26}$) with FGS and Pt@FGS is 63.5 kcal/mol and 57.3 kcal/mol, respectively (the ReaxFF MD simulation results in the same research are 54.0 kcal/mol and 32.3 kcal/mol, respectively) [17]. These values validate the effectiveness of data from the present research.

4. Conclusions

A series of ReaxFF MD simulations are performed to investigate the catalytic mechanisms and kinetics of methane oxidation mixed with Pt/graphene-based nanoparticle additives. The results indicate that Pt@FGS is the most effective catalyst among all the nanoparticle candidates involved in this research. Compared with pure methane oxidation, the combination of Pt and FGS in the Pt@FGS reaction enhances the catalytic activity by dramatically lowering the activation energy by approximately 73%. Moreover, FGS is further oxidized especially at the edge of the graphene sheet during the reaction to increase the functionality. More importantly, the enhanced dehydrogenation of Pt@FGS and interatomic exchanges, rather than the creation of new reactions to form new species, dominate the catalytic process and drive the catalytic cycle involving a wide range of intermediate products. Additionally, the species analysis demonstrates that the catalytic methane oxidation is initiated by the cleavage of C–H bond and the production of hydroxyl. All the graphene-containing structures are monitored throughout the simulation and no destruction of graphene structures is observed. It is worth noting that in the presence of FGS, the nanoparticle exerts a negative impact on methane oxidation at the late stage of the reaction due to the limited activity of active sites on FGS during that time period. This research sheds new light on the catalytic mechanisms for enhanced fuel combustion in the presence of Pt@FGS.

Acknowledgements

Funding from the UK Engineering and Physical Sciences Research Council under the projects "UK Consortium on Mesoscale Engineering Sciences (UKCOMES)" (Grant Nos. EP/L00030X/1 and EP/R029598/1) and "High Performance Computing Support for United Kingdom Consortium on Turbulent Reacting Flow (UKCTRF)" (Grant No. EP/K024876/1) is gratefully acknowledged. The first author is grateful for the Graduate Research Scholarship and Overseas Research Scholarship from University College London. Helpful discussions with Dr. Qian Mao of Tsinghua University are also acknowledged.

Supplementary materials

Supplementary material associated with this article can be found, in the online version, at doi:10.1016/j.proci.2018.05.109.

References

[1] M.J. Allen, V.C. Tung, R.B. Kaner, *Chem. Rev.* 110 (2010) 132–145.
[2] K.S. Novoselov, V.I. Fal'ko, L. Colombo, P.R. Gellert, M.G. Schwab, K. Kim, *Nature* 490 (2012) 192–200.
[3] S. Isert, L. Xin, J. Xie, S.F. Son, *Combust. Flame* 183 (2017) 322–329.
[4] S. Moussa, V. Abdelsayed, M.S. El-Shall, *Chem. Phys. Lett.* 510 (2011) 179–184.
[5] J.L. Sabourin, D.M. Dabbs, R.A. Yetter, F.L. Dryer, I.A. Aksay, *ACS Nano* 3 (2009) 3945–3954.
[6] K.K. Kuo, G.A. Risha, B.J. Evans, E. Boyer, in: MRS Proceedings, 2011, p. 800.
[7] R.A. Yetter, G.A. Risha, S.F. Son, *Proc. Combust. Inst.* 32 (2009) 1819–1838.
[8] J.A. Badra, A.R. Masri, *Combust Flame* 159 (2012) 817–831.
[9] G.G. Martens, G.B. Marin, J.A. Martens, P.A. Jacobs, G.V. Baroni, *J. Catal.* 195 (2000) 253–267.

[10] P. Gelin, L. Urfels, M. Primet, E. Tena, *Catal. Today* 83 (2003) 45–57.
[11] E.H. Jo, H. Chang, S.K. Kim, et al., *Sci. Rep. UK* (2016) 6.
[12] T. Shimizu, A.D. Abid, G. Poskrebyshev, et al., *Combust. Flame* 157 (2010) 421–435.
[13] V. Zhukov, A. Kong, in: Seventh European Conference for Aeronautics and Space Sciences, Mailand, Italien, 2017.
[14] Q. Mao, A.C.T. van Duin, K.H. Luo, *Proc. Combust. Inst.* 36 (2017) 4339–4346.
[15] L.M. Liu, R. Car, A. Selloni, D.M. Dabbs, I.A. Aksay, R.A. Yetter, *J Am Chem Soc* 134 (2012) 19011–19016.
[16] C.Y. Zhang, Y.S. Wen, X.G. Xue, *ACS Appl. Mater. Inter.* 6 (2014) 12235–12244.
[17] H.S. Sim, *Understanding the Role of Multifunctional Nanoengineered Particulate Additives on Supercritical Pyrolysis and Combustion of Hydrocarbon Fuels/Propellants*, The Pennsylvania State University, Pennsylvania, USA, 2016 Ph.D. thesis.
[18] A.C.T. van Duin, S. Dasgupta, F. Lorant, W.A. Goddard, *J. Phys. Chem. A* 105 (2001) 9396–9409.
[19] K. Chenoweth, A.C.T. van Duin, W.A. Goddard, *J Phys Chem A* 112 (2008) 1040–1053.
[20] T.P. Senftle, S. Hong, M.M. Islam, et al., *NPJ Comput. Mater.* 2 (2016) 15011.
[21] J.E. Mueller, A.C.T. van Duin, W.A. Goddard, *J. Phys. Chem. C* 114 (2010) 4939–4949.
[22] Y.K. Shin, L. Gai, S. Raman, A.C.T. van Duin, *J. Phys. Chem. A* 120 (2016) 8044–8055.
[23] S. Plimpton, *J. Comput. Phys.* 117 (1995) 1–19.
[24] I. Fampiou, A. Ramasubramaniam, *J. Phys. Chem. C* 116 (2012) 6543–6555.
[25] G.M. Yang, X.F. Fan, S. Shi, H.H. Huang, W.T. Zheng, *Appl. Surf. Sci.* 392 (2017) 936–941.
[26] F. Castro-Marcano, A.M. Kamat, M.F. Russo, A.C.T. van Duin, J.P. Mathews, *Combust. Flame* 159 (2012) 1272–1285.
[27] K. Chenoweth, A.C.T. van Duin, S. Dasgupta, W.A. Goddard, *J. Phys. Chem. A* 113 (2009) 1740–1746.
[28] M. Dontgen, M.D. Przybylski-Freund, L.C. Kroger, W.A. Kopp, A.E. Ismail, K. Leonhard, *J. Chem. Theory Comput.* 11 (2015) 2517–2524.
[29] Q. Mao, A.C.T. van Duin, K.H. Luo, *Carbon* 121 (2017) 380–388.
[30] W. Humphrey, A. Dalke, K. Schulten, *J. Mol. Graph Model* 14 (1996) 33–38.
[31] B. Szczesniak, J. Choma, M. Jaroniec, *Adv. Colloid Interfac.* 243 (2017) 46–59.
[32] R.K. Chouhan, K. Ulman, S. Narasimhan, *J. Chem. Phys.* (2015) 143.
[33] N. Kariya, A. Fukuoka, M. Ichikawa, *Appl. Catal. A Gen.* 233 (2002) 91–102.
[34] A.B. Mhadeshwar, P. Aghalayam, V. Papavassiliou, D.G. Vlachos, *Proc. Combust. Inst.* 29 (2002) 997–1004.
[35] M. Reinke, J. Mantzaras, R. Schaeren, R. Bombach, A. Inauen, S. Schenker, *Combust. Flame* 136 (2004) 217–240.
[36] M. Reinke, J. Mantzaras, R. Bombach, S. Schenker, A. Inauen, *Combust. Flame* 141 (2005) 448–468.
[37] O. Deutschmann, R. Schmidt, F. Behrendt, J. Warnatz, *Proc. Combust. Inst.* 1–2 (1996) 1747–1754.
[38] R. Quiceno, J. Perez-Ramirez, J. Warnatz, O. Deutschmann, *Appl. Catal. A Gen.* 303 (2006) 166–176.
[39] S.B. Tang, Z.X. Cao, *Phys. Chem. Chem. Phys.* 14 (2012) 16558–16565.
[40] M.D. Salazar-Villalpando, A.C. Miller, *Chem. Eng. J.* 166 (2011) 738–743.
[41] D.P. Serrano, J.A. Botas, J.L.G. Fierro, R. Guil-Lopez, P. Pizarro, G. Gomez, *Fuel* 89 (2010) 1241–1248.
[42] J. Sirijaraensre, J. Limtrakul, *Phys. Chem. Chem. Phys.* 17 (2015) 9706–9715.
[43] F.L. Dryer, I. Glassman, *Proc. Combust. Inst.* 14 (1973) 987–1003.
[44] J.B. Fenn, H.F. Calcote, *Proc. Combust. Inst.* 4 (1953) 231–239.
[45] C.K. Westbrook, F.L. Dryer, *Combust. Sci. Technol.* 27 (1981) 31–43.
[46] R. Abbasi, L. Wu, S.E. Wanke, R.E. Hayes, *Chem. Eng. Res. Des.* 90 (2012) 1930–1942.
[47] J.G. Firth, H.B. Holland, *Trans. Farad. Soc.* 65 (1969) 1121–1127.
[48] K. Otto, *Langmuir* 5 (1989) 1364–1369.